Sodium Cyclopentadienide as a New Type of Electrolyte for Sodium Batteries

Markus Binder[+],[a] Magdalena Mandl[+],*[a] Steve Zaubitzer,[b] Margret Wohlfahrt-Mehrens,[a, b] Stefano Passerini,[a] Olaf Böse,[a, b] Michael A. Danzer,[c, d] and Mario Marinaro[b]

Owing to the low cost and high abundance of sodium, sodium-based batteries, especially those employing metallic sodium anodes, are considered for post-lithium energy storage. In order to develop high-performance and long-lasting sodium-metal batteries, however, the reversible Na-metal stripping and plating challenge must be addressed. Most organic electrolytes suffer from non-uniform and continuous formation of the solid electrolyte interphase as well as unfavorable dendritic growth. The use of sodium cyclopentadienide dissolved in tetrahydrofuran as the electrolyte reveals an improved reversibility of sodium dissolution and electrodeposition combined with an electrochemical stability window of around 2.2 V vs. Na/Na^+ and an ionic conductivity of 1.36 mS cm^{-1} at 25 °C. Furthermore, the plated electrodes showed a remarkable morphology of the Na deposits, that is, no dendrite formation, whereby the above-mentioned electrolyte could overcome the aforementioned cycling issues, thus suggesting suitability for further studies.

Owing to the growing demand on energy storage systems, besides the today's commercially used lithium-ion batteries (LiBs), sodium batteries have become a topic of interest. The economic factors, like wide occurrence and good accessibility of sodium, eliminate geopolitical issues and therefore open opportunities for its application in post-lithium energy storage batteries. In fact, the European Union ranks sodium batteries as important technology to establish for the future battery market.[1,2] Due to its low cost, sodium is recognized as a future candidate for large-scale energy storage systems to better integrate renewable energy into the grid.[3,4]

Since the chemical properties of lithium and sodium are similar, investigations often focus on transferring the insights of LiBs into the development of sodium-ion battery technologies. The overall lower performance compared to LiBs is a consequence of the more positive redox potential (sodium: −2.71 V vs. SHE (standard hydrogen electrode); lithium: −3.04 V vs. SHE), limiting the voltage range at the negative electrode to avoid metal deposition. Also, its larger ionic radius (1.02 Å for Na^+ vs. 0.76 Å for Li^+) results into sluggish reaction kinetics.[5,6] Moreover, Na has a higher atomic weight than Li, resulting in a lower specific capacity. Therefore, sodium-ion batteries (SIBs) still require further improvements of the electrolyte and electrode materials in order to concur with established energy storage systems. One way to improve the energy density of sodium batteries consists in using sodium metal (or its alloys) as the negative electrode (anode material) instead of insertion materials, since the metal can provide high theoretical capacity (1165 mAh/g) and rather negative potential (i.e., −2.71 V vs. SHE).[7] A similar approach is under extensive investigation for lithium metal batteries because of the same advantages. Unfortunately, both alkali metal anodes show similar problems in batteries, namely, large volume changes, electrolyte consumption (solid electrolyte interphase (SEI) formation) and dendritic growth upon charge.[7–9] In contrast to lithium metal anodes, in which a dense inorganic SEI at the electrode/electrolyte interface forms during the first cycles and mitigates continuous electrolyte decomposition,[9] the SEI on sodium is reported to be less stable, e.g. the inorganic SEI's components are more soluble in the electrolyte.[8,11] Consequently, the SEI grows continuously upon cycling (or rather more strongly).[12] To overcome these issues, the interaction of the metal electrode with the electrolyte is believed to be a key factor. Therefore, the introduction of new electrolytes may lead to the necessary changes in electrochemical sodium dissolution and deposition, commonly referred to as stripping and plating behavior. The studies of the stripping and plating behavior are not just interesting for metallic anodes. In fact, they can also help to improve the performance of insertion materials since stripping and plating processes may occasionally occur on their surface, especially for higher current densities at lower temperatures.[13]

Inspired by the work of Schwarz et al. on $Mg(Cp)_2$ based electrolyte,[14] which reported remarkable performance for the electrochemical Mg plating/stripping, we herein present a novel

[a] M. Binder,[+] M. Mandl,[+] Dr. M. Wohlfahrt-Mehrens, Prof. Dr. S. Passerini, Dr. O. Böse
Helmholtz Institute Ulm (HIU) Electrochemical Energy Storage
Helmholtz Str. 11, 89081 Ulm, Germany
E-mail: magdalena.mandl@kit.edu
[b] S. Zaubitzer, Dr. M. Wohlfahrt-Mehrens, Dr. O. Böse, Dr. M. Marinaro
Centre for Solar Energy and Hydrogen Research Baden-Württemberg (ZSW)
Helmholtz Str. 8, 89081 Ulm, Germany
[c] Prof. Dr.-Ing. M. A. Danzer
University of Bayreuth
Chair of Electrical Energy Systems (EES)
Universitätsstr. 30, 95447 Bayreuth, Germany
[d] Prof. Dr.-Ing. M. A. Danzer
Bavarian Center for Battery Technology (BayBatt)
Universitätsstr. 30, 95447 Bayreuth, Germany
[+] These authors contributed equally to this work

Supporting information for this article is available on the WWW under https://doi.org/10.1002/celc.202001290

electrolyte for Na plating/stripping based on a similar concept. In this work the electrolyte constituted by a 2 M solution of sodium cyclopentadienide (NaCp) in tetrahydrofuran (THF), is investigated in symmetrical sodium metal cells. In particular, cyclic voltammetry (CV), electrochemical impedance spectroscopy (EIS), and *ex-situ* scanning electron microscopy (SEM) with energy-dispersive X-ray spectroscopy (EDX) of the electrodes, have been used to investigate the stripping/plating behavior and the electrolyte conductivity of the above mentioned cells.

The determined ionic conductivity of 1.36 mS cm^{-1} at 25 °C does not reach the conductivities of standard electrolytes for LiBs or the corresponding sodium electrolyte, i.e., the solution of $NaPF_6$ in different carbonate-based solvents (~ 10 mS cm^{-1}[15,16]). Nonetheless, the Arrhenius plot in Figure 1 shows a sufficient ionic conductivity in the temperature range of 0 °C–50 °C, which undergoes just small temperature dependent changes. For sub-zero temperatures the conductivity shows a leap and a change of slope. These result in a significant lower conductivity and could thereby limit the applicable temperature range for the electrolyte. Similar behavior is known from $NaPF_6$ and $LiPF_6$,[15] which also show a significant lower ionic conductivity with decreasing temperatures.

The feasibility of NaCp as electrolyte salt, i.e., the prove of charge transfer in an electrochemical cell, has been investigated assembling cells consisting of sodium metal and copper metal electrodes. The obtained eye-visible deposits on the Cu electrode were investigated by SEM and EDX (SI). The results prove the plating of pure metallic sodium as detected by EDX. The reversibility of the sodium stripping and plating was studied by cyclic voltammetry (Figure 2 a) using a scan rate of 5 mVs^{-1}. Over a set of 40 cycles, the cell showed a coulombic efficiency of 90.9% during the initial cycles, which increased up to 96.4% during cycle 40. Cycling in the potential range from −0.3 V to 1 V versus Na/Na^+ revealed a very reproducible current response. The cathodic scans showed no side reactions and the onset of sodium plating showed no significant overpotential. At the cathodic cut-off potential of −0.3 V a peak current density of around 5.5 mA cm^{-2} is reached. Moreover, the anodic scans showed no overpotential and a maximum current density of 4 mA cm^{-2} at 0.3 V. Besides the slightly tailed peak shape caused by diffusion, which leads to a current density of ~0.5 mA cm^{-2} at the anodic cut-off potential of 1 V, there are no indicators for further limitations of the reaction.

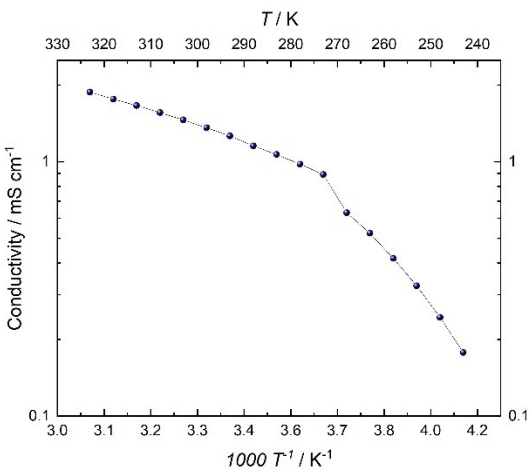

Figure 1. Arrhenius plot of the ionic conductivity in a temperature range from −30 °C to 50 °C (continuous line to guide the eye).

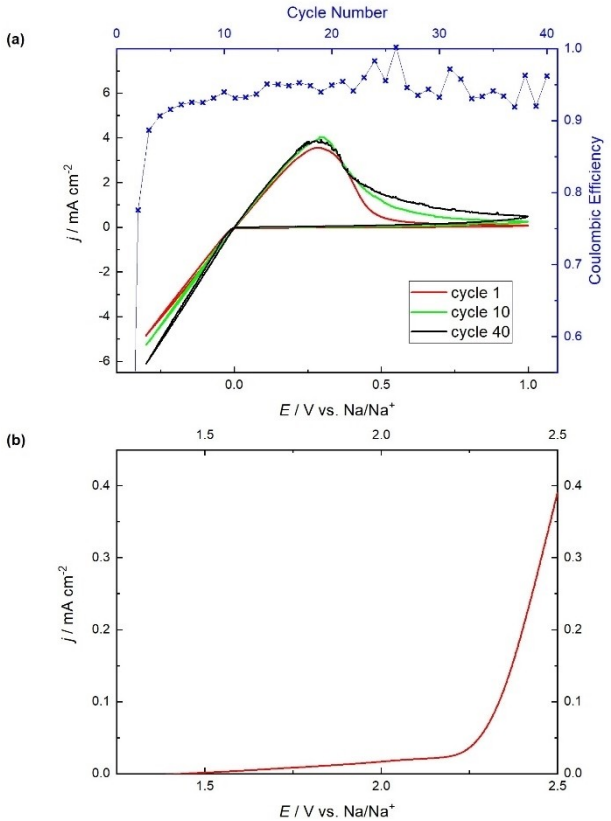

Figure 2. Electrochemical characterization of the 2 M NaCp/THF electrolyte. a) Cyclovoltammetry and the corresponding coulombic efficiencies for the sodium electrodeposition/dissolution process using Cu as the working electrode and Na as counter and reference electrodes. Scan rate 5 mV s^{-1}. b) Linear sweep voltammetry on Cu at a scan rate of 5 mV s^{-1}. Reference and counter electrodes: Na.

Linear sweep voltammetry (LSV) experiments at different scan rates were performed to obtain the electrochemical stability window (ESW). Defining 10 μA cm^{-2} as the decomposition threshold,[17] results in an anodic stability of around 2.25 V vs. Na/Na^+. Since THF (solvent) is stable up to around 3.7 V,[18] the stability of the cyclopentadienide anion limits the ESW.

One major novelty of the NaCp electrolyte is the potential response during constant-current (CC) experiments. The typical result of a 0.5 h CC-step with a current density of 0.4 mA cm^{-2} is shown in Figure 3 b. It shows a logarithmic trace, meaning that the overpotential of the given CC-step increases just slowly over time. In comparison, Figure 3 b shows the typical potential response of a cell with $NaPF_6$ electrolyte (in EC : DMC 1 : 1) under the same CC conditions. This type of potential curve was observed not only during our studies with $NaPF_6$ and $NaClO_4$ (supporting information and[11]), but also in previous studies on lithium metal anodes using different electrolytes.[19–21]

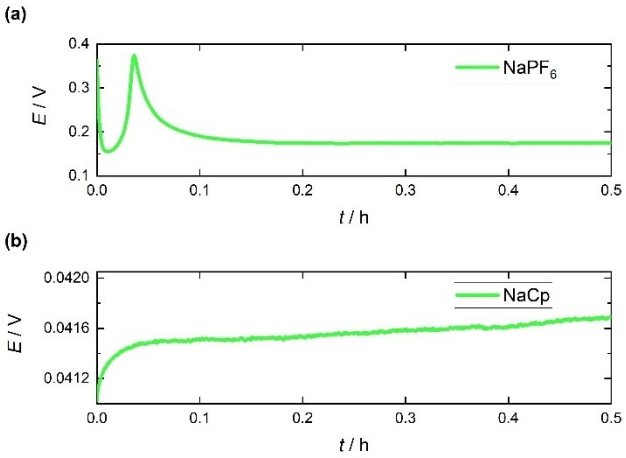

Figure 3. Examples of typical potential curves for symmetric sodium cells under constant current conditions (Icc = 0.4 mA cm^{-2}). a) 1 M $NaPF_6$ electrolyte in EC:DMC (1:1). b) 2 M NaCp electrolyte in THF.

In such a curve, the sharp peak shortly after applying the current correlates with the high initial activation barrier for stripping from the bulk or plating onto an unaffected surface. Its decay is due to the lower barrier for the stripping and plating processes on already existing structures (pits and dendrites, respectively). Overall, such potential curves are typical for mossy dendritic growth.[20,21] The absence of this peak in the potential response of the NaCp cell indicates that there is no such energy benefit stripping from pits and plating onto existing dendrites/electrodeposits. Thereby, NaCp could prevent the ongoing growth of these structures and enable a more homogenous sodium deposition even after continuous cycling. It is worth noting that the plateau for the $NaPF_6$ electrolyte cell, which adjusts after about 0.1 h, occurs at a ~5 times higher potential than that of the NaCp electrolyte cell (200 mV compared to ~40 mV respectively). This very low overpotential for NaCp suggests a lower activation barrier for the electrochemical stripping and plating and represents a huge advantage compared to the other electrolytes (namely, $NaPF_6$ and $NaClO_4$). During a set of 15 cycles, consisting of the before mentioned CC-steps with alternating sign, electrochemical impedance spectroscopy was performed after each cycle (SI Figure 1). This shows that the electrolyte resistance, given by the real axis intersection,[22] increases by over 25% during cycling. This observation is also visible in the 25% higher voltage response in the CC steps, most probably pointing to the ongoing electrolyte consumption.

Nonetheless, the polarization of the NaCp cell increases during cycling (SI Figure 1), slightly up to the 10th cycle, and about 5% per cycle from 10th cycle on. This can be explained by the ongoing SEI growth, which consumes the electrolyte leading to an increasing polarization resistance. In addition, the cell dries out (due to the electrolyte consumption) and therefore the resistance at the interface electrolyte/electrode increases.

To investigate the surface morphology of the sodium electrodes, *ex-situ* SEM analysis was performed. Figure 4 shows typical images of electrodeposits (a and c) and pits (b and d) formed on the Na electrode in NaCp electrolyte, each with a close up (a and b) and an overview picture (c and d). The electrode which was stripped during the last cycle normally shows exclusively pits were as the electrode plated during the

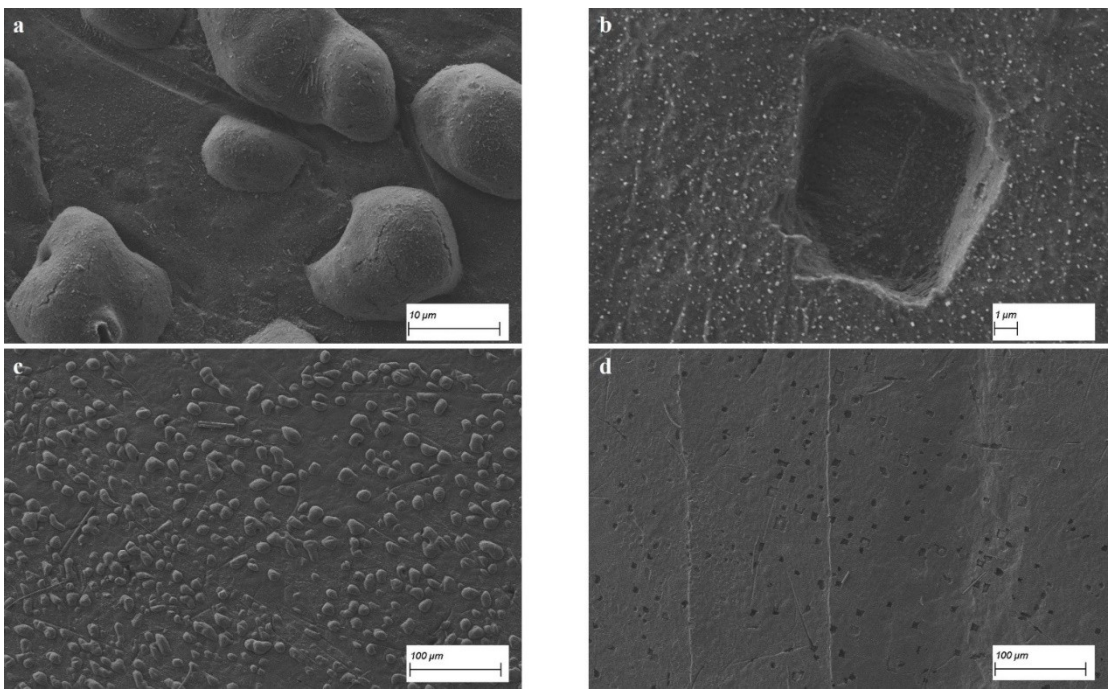

Figure 4. SEM images of the globular electrodeposits (a, c) and pits (b, d) formed on Na metal electrodes after three cycles using the NaCp electrolyte (EHT = 3 kV, WD = 5.0 mm, SE2 detector).

last cycle only exhibits the deposits. This finding indicates that structures from previous cycles are mostly removed, i.e., pits are filled, and deposits are dissolved before the formation of new pits and deposits begins. This assumption is confirmed by the size of these structures which lies in the range of a couple of micrometers (1–10 μm) and the fact that they do not get larger with increasing cycle number (see SI Figure 5; compare with growing dendrites in $NaPF_6$[11]). Furthermore, the number of pits and electrodeposits is more or less constant throughout cycling. In our earlier studies with $NaPF_6$ and $NaClO_4$, the electrodes always contained both, pits and dendrites, independent of the current direction during the last cycle. Additionally, the size in those other electrolytes is normally much larger and lies in the range of a few hundred micrometers (for further information to the other electrolytes, including SEM images, see SI). With the presented SEM findings, we can consolidate that the electrodeposition and dissolution processes are more reversible in the NaCp-based electrolyte, promoting a more homogeneous electrode surface during cycling. This homogeneous surface should then be able to enhance the long-term cycling performance of the given system.

Additionally, the deposits in Figure 4 a) show a remarkable morphology: round and smooth. This morphology was not documented for sodium before, but is similar to, e.g., magnesium plating in ionic liquid based electrolytes.[23] In other sodium electrolytes (e.g., SI Figure 5–9), however, mossy structures are identified, which can probably lead to dead sodium and thereby lower the efficiency significantly.[24] On the other hand, the globular electrodeposits obtained in the NaCp-based electrolyte represent a possible improvement in another aspect as well.

Overall, the herein reported NaCp electrolyte shows an electrochemical stability window of about 2.2 V and thereby is feasible for low voltage cells such as Na/S systems. The ionic conductivity of this new Na-ion electrolyte ranges in the same order of magnitude as those employing $NaPF_6$ or $NaClO_4$ electrolytes, i.e., similar to the conventional electrolytes for LiBs. The NaCp electrolyte enables reversible cycling for the symmetric Na cells, even though a clear increase of the electrolyte resistance is observed along the performed 15 cycles. A further advantage of the NaCp electrolyte is the rather low overpotential, indicating an easy charge transfer at the electrode/electrolyte interface. In total, the electrochemical stripping and plating behavior appears interesting and worth further investigations. The homogeneous surface deposition, i.e., non-mossy electrodeposits, could, actually, lead to enhancements of the cycle life and coulombic efficiency of Na metal batteries employing such an electrolyte.

Experimental Section

For all experiments, the samples were handled under inert atmosphere in a glovebox with a typical oxygen and water content below 0.1 ppm.

Materials: dry stick sodium (>99.8%, Acros organics), sodium cyclopentadienide (2 M in THF, Sigma Aldrich, used as purchased, determined water content ~150 ppm), glass fiber separator (Whatman grade GF/D).

Equipment: Swagelok-type, three-electrode cells (potentiodynamic measurements), ECC-PAT-Core housings from EL-Cell (constant current measurements), Solartron Analytical 1470E/1485 A cell testing system, ESPEC PI-2 K climate chamber, Zeiss Crossbeam 340 FIB-SEM.

The ionic conductivity was determined by the automated multiplexed conductivity meter equipped with a frequency analyzer and a thermostatic chamber (MCS-10, Bio-Logic).

Further experimental details are included in the supporting information.

Acknowledgements

This work contributes to the research performed at CELEST (Center for Electrochemical Energy Storage Ulm-Karlsruhe). The HIU authors acknowledge the funding from the Helmholtz Association. S.P. acknowledges the Bundesministerium für Bildung und Forschung (BMBF) in the framework of TRANSITION project (FKZ 03XP0186A). S.Z., M.M. and M.W.-M. kindly acknowledge the financial support of the Bundesministerium für Bildung und Forschung (BMBF) in the framework of MeLuBatt project (FKz 03XP0110E) and the German Research Foundation (DFG) under Project ID 390874152 (POLiS Cluster of Excellence). Furthermore, we would like to thank Ivana Hasa and Hanno Schütz for their help with the potentiodynamic and the conductivity measurements. Open access funding enabled and organized by Projekt DEAL.

Conflict of Interest

The authors declare no conflict of interest.

Keywords: electrochemistry · electrolytes · sodium-ion batteries · sodium cyclopentadienide · metal deposition and dissolution

[1] *The Strategic Energy Technology (SET) Plan*, European Commission, **2018**.
[2] Science for Environment Policy, *Towards the Battery of the Future*, Produced For The European Commission DG Environment By The Science Communication Unit, UWE, Bristol, **2018**.
[3] C. Vaalma, D. Buchholz, M. Weil, S. Passerini, *Nat. Rev. Mater.* **2018**, *3*, 18013.
[4] M. Baumann, J. F. Peters, M. Weil, A. Grunwald, *Energy Technol.* **2017**, *5*, 1071–1083.
[5] L. Li, Y. Zheng, S. Zhang, J. Yang, Z. Shao, Z. Guo, *Energy Environ. Sci.* **2018**, *11*, 2310–2340.
[6] K. Kubota, S. Komaba, *J. Electrochem. Soc.* **2015**, *162*, A2538–A2550.
[7] X. Zheng, C. Bommier, W. Luo, L. Jiang, Y. Hao, Y. Huang, *Energy Storage Mater.* **2019**, *16*, 6–23.
[8] G. Bieker, M. Winter, P. Bieker, *Phys. Chem. Chem. Phys.* **2015**, *17*, 8670–8679.
[9] X. B. Cheng, R. Zhang, C. Z. Zhao, F. Wei, J. G. Zhang, Q. Zhang, *Adv. Sci.* **2015**, *3*, 1–20.
[10] B. Lee, E. Paek, D. Mitlin, S. W. Lee, *Chem. Rev.* **2019**.
[11] M. Mandl, J. Becherer, D. Kramer, R. Mönig, T. Diemant, R. J. Behm, M. Hahn, O. Böse, M. A. Danzer, *Electrochim. Acta* **2020**, 136698.

[12] Z. W. Seh, J. Sun, Y. Sun, Y. Cui, *ACS Cent. Sci.* **2015**, *1*, 449–455.
[13] Q. Liu, C. Du, B. Shen, P. Zuo, X. Cheng, Y. Ma, G. Yin, Y. Gao, *RSC Adv.* **2016**, *6*, 88683–88700.
[14] R. Schwarz, M. Pejic, P. Fischer, M. Marinaro, L. Jörissen, M. Wachtler, *Angew. Chem. Int. Ed.* **2016**, *55*, 14958–14962; *Angew. Chem.* **2016**, *128*, 15182–15186.
[15] D. I. Iermakova, R. Dugas, M. R. Palacín, A. Ponrouch, *J. Electrochem. Soc.* **2015**, *162*, A7060–A7066.
[16] A. Ponrouch, E. Marchante, M. Courty, J. M. Tarascon, M. R. Palacín, *Energy Environ. Sci.* **2012**, *5*, 8572–8583.
[17] L. G. Chagas, S. Jeong, I. Hasa, S. Passerini, *ACS Appl. Mater. Interfaces* **2019**, *11*, 22278–22289.
[18] S. A. Campbell, C. Bowes, R. S. McMillan, *J. Electroanal. Chem.* **1990**, *284*, 195–204.
[19] K. N. Wood, M. Noked, N. P. Dasgupta, *ACS Energy Lett.* **2017**, *2*, 664–672.
[20] Y. Deng, J. Zheng, A. Warren, J. Yin, S. Choudhury, P. Biswal, D. Zhang, L. A. Archer, *Adv. Energy Mater.* **2019**, *9*, 1–9.
[21] K. N. Wood, E. Kazyak, A. F. Chadwick, K. H. Chen, J. G. Zhang, K. Thornton, N. P. Dasgupta, *ACS Cent. Sci.* **2016**, *2*, 790–801.
[22] S. Schindler, *PhD Thesis, Univ. Bayreuth* **2018**.
[23] X. Gao, A. Mariani, S. Jeong, X. Liu, X. Dou, M. Ding, A. Moretti, S. Passerini, *J. Power Sources* **2019**, *423*, 52–59.
[24] J. Steiger, D. Kramer, R. Mönig, *Electrochim. Acta* **2014**, *136*, 529–536.

Manuscript received: October 5, 2020
Accepted manuscript online: October 26, 2020